

MAGNETIC RESONANCE TECHNIQUES

Solid State NMR Studies in Polyolefins

Alamo, R.G., FAMU-FSU College of Engineering
VanderHart, D., National Institute of Standards and Technology

Huang, W.T., FAMU-FSU College of Engineering

Solid state NMR studies of polypropylenes and polyethylenes have been performed within three ongoing research programs in our laboratory.

The first program focuses in understanding the partitioning of the defects of the polypropylene molecule among the different phases of the lamellar crystallite. Homo-polypropylenes and different types of random propylene copolymers have been studied and resonances associated with the defects in the crystallite regions have been identified directly by CP MAS ^{13}C NMR, as well as theoretically by quantum chemical computations. This work has been carried out in collaboration with Dr. D. VanderHart of the National Institute of Standards and Technology (NIST). The NMR spectra were acquired at NIST and with the Bruker 300 MHz of the NHMFL. Two main papers have been published in *Macromolecules* and the work has been presented in different meetings of the American Chemical and Physical Societies.

A second program is directed toward understanding the conformational and dynamic properties that cause profound melting kinetics in the fusion of polypropylene crystals. This work is part of Ms. W.T. Huang's Ph.D. thesis. Spin lattice relaxation (T_{1H}) in the interlamellar amorphous region are measured, aiming to understand relaxation and conformational properties of this region. The experiments are carried out in the Bruker 300 MHz spectrometer. Polypropylenes with different defects are crystallized for different lengths of time and the T_{1H} was measured. These studies will test the interplay between entropic changes in the interlamellar constrained regions during crystallization and specific lamellar morphologies.

In a third program, the nature of the structural changes that take place with time upon annealing rapidly crystallized polyethylenes is assessed in relation to their initial crystalline morphology. The conformational dynamics of the intercrystalline region are followed through the evolution of the spin-lattice relaxation in this region. These experiments are carried out in the wide bore Bruker DRX 500 MHz spectrometer housed in the FAMU-FSU College of Engineering.

Detection of Spin Labels in Aqueous Solutions by HFEPR

Bauman, B., NHMFL/FSU, Biological Sciences

Fajer, P., NHMFL/FSU, Biological Sciences

Saylor, C.A., NHMFL

Maresch, G.G., NHMFL

Brunel, L.-C., NHMFL

Aqueous solutions are the essential environment for biologically relevant samples. Enzymes and proteins are commonly dissolved in buffers for pH stabilization. This has been a challenge for EPR instrumentation for decades because the microwave radiation is strongly scattered by water. For conventional low-frequency measurements, the samples are placed in thin flat cells at nodes of the electrical field in the probe to minimize the effect of microwave absorption. For higher frequencies, with wavelengths on the order of millimeters, new ways of sample preparation and placement in the probe are required.

The EPR spectrum shown in Fig. 1 represents a significant step to proving how the current quasi-optical EPR continuous-wave (CW) spectrometer can be used for the detection of aqueous biological samples. The achieved signal-to-noise ratio from a one millimolar concentration of the nitroxide radical TEMPO (2,2,6,6-tetramethyl-1-piperidine-N-oxyl) in 70 % glycerol in water at room temperature and 220 GHz is sufficient for high-resolution EPR studies of spin labeled proteins. Chemically equivalent molecules are commonly used for spin labeling of proteins. It is important to note that for the measurement of spectrum in

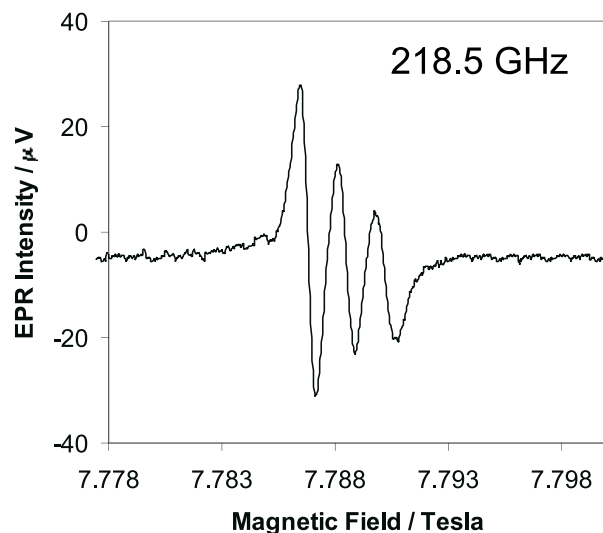


Figure 1. High-frequency EPR spectrum of a nitroxide spin label in 70 % glycerol in water detected at 218.5 GHz.

Fig. 1., a non-resonant probe was used. The sample was placed in a container that restricted the liquid to stay flat in a thin layer on the reflecting mirror at the end of the microwave transmission line. The layer thickness was about 150 micrometers. This thickness is an optimum for the compromise between the reduction of microwave absorption by using thinner layers and the increase of the number of electron spins by using a larger sample volume.

For low loss samples, the spectrometer sensitivity is of $3 \cdot 10^{10}$ spins per Gauss. $(\text{Hz})^{1/2}$, this is eight times better than the sensitivity derived from the signal-to-noise ratio of the spectrum in Fig. 1. This factor of eight is due to the strong scattering effect of the solvent. In resonant cavities, the difference in sensitivity between non lossy and aqueous samples can be an order of magnitude larger than this factor of eight. As a result, at high frequencies essentially the use of a non resonant probe enables the measurement of low concentrated spin labels.

Acknowledgements: This work was supported by NSF grant 5024-54522.

PISEMA Powder Patterns and PISA Wheels

Denny, J.K., Mercer Univ., Mathematics
 Wang, J., FSU, Molecular Biophysics
 Cross, T.A., NHMFL, Chemistry and Institute for
 Molecular Biophysics
 Quine, J.R., FSU, Mathematics

Resonance patterns observed in 2D solid-state NMR from a transmembrane alpha helix have been demonstrated^{1,2} to yield structural details of the protein. The PISEMA (polarization inversion spin exchange at magic angle) experiment correlates anisotropic dipolar and chemical shift interactions for ¹⁵N labeled proteins. The patterns observed have been termed PISA wheels. These wheels are useful both in assigning the resonances and in determining the orientation of the helix with respect to the magnetic field.

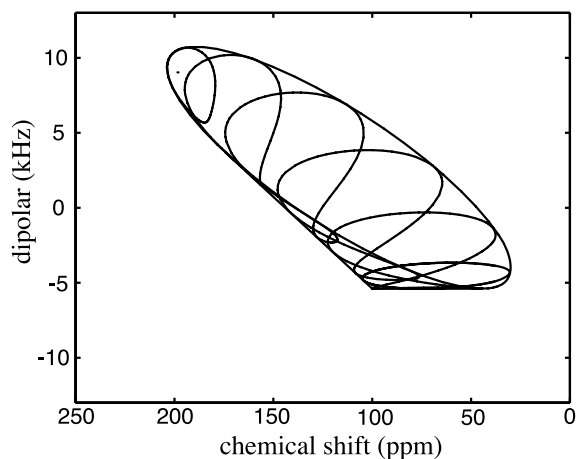


Figure 1. The singlet powder pattern is the union of the PISA wheels.

We give a mathematical discussion of the PISEMA powder spectrum. This spectrum is given as the image in the frequency plane of a quadratic function from the sphere of unit vectors. The simplicity of this function allows easy calculation of the powder spectrum, and a change of variables to a helix axis frame for the alpha helix gives parametric equations for the PISA wheels. The union of these PISA wheels gives the entire powder spectrum.

¹ Marassi, F.M., *et al.*, *J. Mag. Res.*, **144**, 156-161 (2000).
² Wang, J., *et al.*, *J. Mag. Res.*, **144**, 162-167 (2000).

Double Rotation NMR at High Fields

Gan, Z., NHMFL

Cross, T., NHMFL/FSU, Chemistry and Molecular Biophysics

Samoson, A., National Institute of Chemical Physics and Biophysics, Estonia

Dupree, R., Univ. of Warwick, England, Physics

Derewinski, M., Polish Academy of Sciences

Double rotation (DOR) completely averages the anisotropic line broadening from the second-order quadrupolar effect. It is the most direct approach to high resolution solid state NMR of half-integer quadrupolar nuclei when compared to other methods like dynamic angle spinning, MQMAS, and STMAS. A DOR probe has been developed at the NHMFL in collaboration with Dr. Ago Samoson of the National Institute of Chemical and Biophysics (NICBP) of Estonia. In combination with the high magnetic fields at the NHMFL, the DOR probe provides users with the capability of the highest resolution available for solid state NMR applications of nuclei like ^{17}O and ^{27}Al . Reported here are some initial results and features of the DOR probe.

Fig. 1 shows ^{17}O and ^{27}Al spectra acquired at 17 T demonstrating the high spectral resolution obtained by DOR and high fields. The spectrum of ^{17}O -enriched KTP shows resolved resonance lines for the eight Ti-O-P sites. The ^{27}Al spectrum demonstrates the application of DOR NMR in zeolites. ^{27}Al resonance lines are broadened by the variation of chemical shift among sites in the zeolite frame work and by the quadrupolar interactions. Double rotation eliminates the portion from the second-order quadrupolar effect and improves spectral resolution. Fig. 1 shows a partially resolved ^{27}Al spectrum for the ZSM zeolite sample.

The double rotor, 13 mm in diameter and fitted inside a standard 40 mm probe head, is capable of spinning up to 1500 Hz. Rotor synchronization of pulse sequence eliminates odd number spinning sidebands; therefore, spinning sidebands are at least 3 kHz away. Samples are packed inside a 4 mm inner

rotor that spins more than four times of the outer rotor speed. The new DOR probe adopts a complete air bearing design that avoids mechanical contact of any moving parts. The probe has been tested for a weekend run without any glitch and is robust to operate.

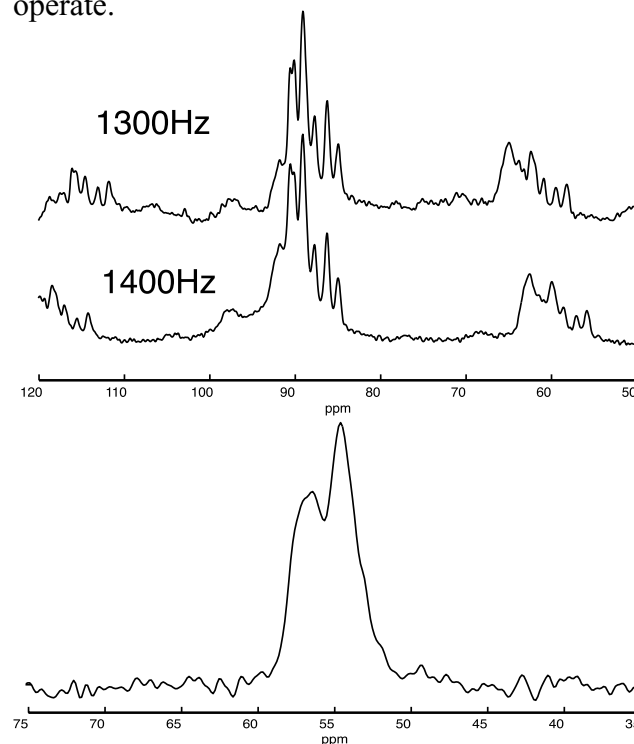


Figure 1. ^{17}O DOR spectra of KTP acquired with two different speeds (top) and ^{27}Al DOR spectrum of a ZSM zeolite sample (bottom).

Probes for 19.6 T (833 MHz) Solid State NMR

Gor'kov, P.L., NHMFL

Gan, Z., NHMFL

Fu, R., NHMFL

Samosan, A., National Institute of Chemical Physics, Estonia

Samoilenko, A., Institute of Chemical Physics, Russia

The NHMFL's high field, 19.6 T (833 MHz), ultra-narrow, 31 mm bore, superconducting magnet is attractive for NMR of solids because of its high field as well as its high stray field gradients. Building NMR probes for this magnet presents a challenge due to the limited space inside its bore and for this reason commercial probes are not readily available. We have developed several NMR instruments for various solid state and imaging applications.

A MAS probe using 4 mm Bruker rotors with spinning speeds up to 10 kHz has been built for low-gamma nuclei. The primary use of this probe is for solid state NMR applications in a variety of solid materials such as glasses, zeolites, or semiconductors, that contain low gamma nuclei such as ^{99}Ru , ^{109}Ag , ^{49}Ti , ^{25}Mg , ^{67}Zn or ^{33}S . High magnetic fields not only provide much needed sensitivity, but higher Larmor frequencies also reduce the probe ring-down time.

A fast 40 kHz MAS probe has been built for high resolution NMR of quadrupolar nuclei with large coupling constants. Under magic-angle spinning, the central transitions of quadrupolar nuclei are broadened by the second-order quadrupolar effect that cannot be averaged by MAS alone. In order to separate spectral overlap from spinning sidebands, MAS frequencies faster than the central transition linewidth are required. Another application of fast MAS is the observation of satellite transitions. Fig. 1 shows the MAS spectrum of Al_9B_2 . For spins 5/2 like that of aluminum, inner satellite transition offers higher spectral resolution than the commonly observed central transitions. The splitting among the four aluminum sites is clearly better seen in the satellite transition spectrum.

A Stray Field Imaging (STRAFI) probe (Fig. 2) has been built for high-resolution stray field imaging of layered structures and for diffusion studies in thin films. It utilizes the unusually high stray field of 75 T/m, available in the 19.6 T magnet at about 12.2 T (520 MHz) plane. This stepper-motor driven probe achieves a slice resolution of 15 to 40 micron for samples up to 10 mm in diameter. Slice selection is made by a vertically aligned RF coil that moves the sample through the observation plane.

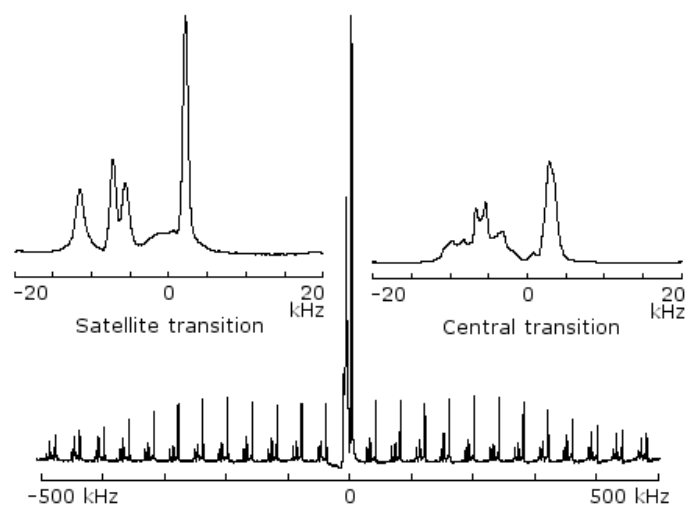


Figure 1. MAS spectrum of Al_9B_2 at 40 kHz spinning speed.

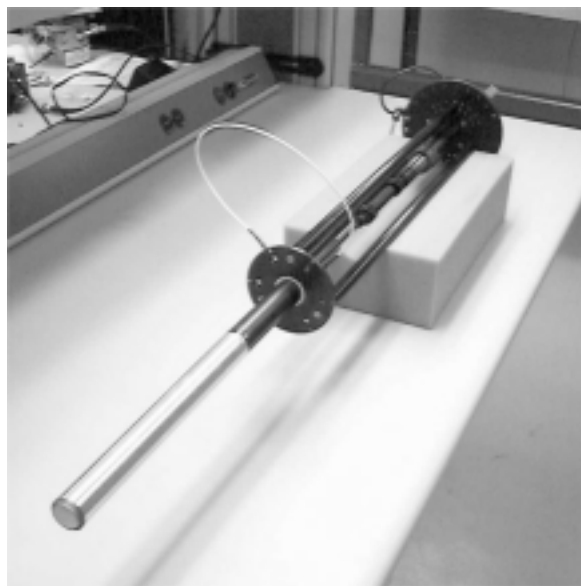


Figure 2. STRAFI probe for 19.6 T (833 MHz) magnet.

Molecular Refinement and Cross-Validation with Solid-State NMR Orientational Data

Kim, S., NHMFL/FSU, Molecular Biophysics
Bertram, R., FSU, Molecular Biophysics
Chapman, M., FSU, Chemistry and Molecular Biophysics
Quine, J., NHMFL/FSU, Mathematics and Molecular Biophysics
Cross, T.A., NHMFL/FSU, Chemistry and Molecular Biophysics

Solid-state NMR is a developing technique for the determination of three-dimensional molecular structures, and has particular promise in the structure determination of membrane proteins and polypeptides. We developed a procedure for using orientational restraints from solid-state NMR in the atomic refinement of molecular structures. Using samples that have uniformly aligned molecules in a lipid bilayer, the measurements of dipolar and quadrupolar couplings and chemical shifts provide orientational restraints for the molecular frame of atomic sites with respect to the magnetic field and a unique molecular axis.

The software CNS-SS¹ is in the form of a module to the refinement package, CNS, which utilizes both least-squares and simulated annealing minimization techniques, and is several orders of magnitude faster than previous software, TORC, developed for solid-state NMR refinement.² The refinement with CNS-SS was performed on a DEC Alpha workstation, and required less than a minute of computer time. With the new procedure, computational speed will not be a limiting factor in the structure determination of larger polypeptides or proteins using solid-state NMR. Also, this short computation time is advantageous for resolving problems with a refinement process, such as over-fitting and structural validation. Complete cross-validation and free R calculations are also implemented to check the model quality. The idea of cross-validation using the solid-state NMR data involves partitioning the experimental data into a test set and a working set and checking the free R-value during the refinement process. This approach

is similar to the method used in crystallography and solution NMR.^{3,4} The free R factor, computed by omitting a fraction of the dipolar and quadrupolar coupling and chemical shift data during a refinement, is currently being used to optimize refinement parameters.

¹ Bertram, R., *et al.*, JMR, **147**, 9-16, (2000).

² Ketchum, R.R., *et al.*, Structure, **5**, 1655-1669 (1997).

³ Brunger, A.T., *et al.*, Science, **261**, 328-331 (1993).

⁴ Clore, G.M., *et al.*, J. Am. Chem. Soc., **121**, 9008-9012 (1999).

HF-EPR Concentration Sensitivity Study of Frozen Mn(III) Solutions ▀IHRP▄

Krzystek, J., NHMFL
Telser, J., Roosevelt Univ., Chemistry
Saylor, C., NHMFL
Brunel, L.-C., NHMFL

From a chemical point of view, EPR of frozen solutions is of paramount importance. This is so because (i) many substances, notably of biological origin, cannot be easily crystallized, and (ii) dissolving a sample and freezing it provides the best way of assuring a random distribution of molecules throughout the volume. High frequency and field EPR of frozen solutions of paramagnetic ions is only in its infancy.¹ There are many parameters that need to be tested such as the proper choice of glass, both from the point of view of its dielectric losses at high frequencies, and the concentration sensitivity obtainable in the currently available instrumentation.² The present study addresses both issues for the high-spin Mn(III) ion ($S=2$) in three complexes: the water-soluble mesotetrasulfonatoporphyrinatomanganese(III), MnTSP, as well as acetylacetonato-manganese(III), Mn(acac)₃, and (*R,R*)-(-)-*N,N'*-bis(3,5-di-*tert*-butylsalicylidene)-1,2-cyclohexane-diaminomanganese(III) chloride, also known as Jacobsen's catalyst. The latter two samples are only soluble in organic solvents.

We have been able to obtain excellent quality EPR spectra from both aqueous and non-aqueous frozen solutions of these Mn(III) complexes. Fig. 1 shows

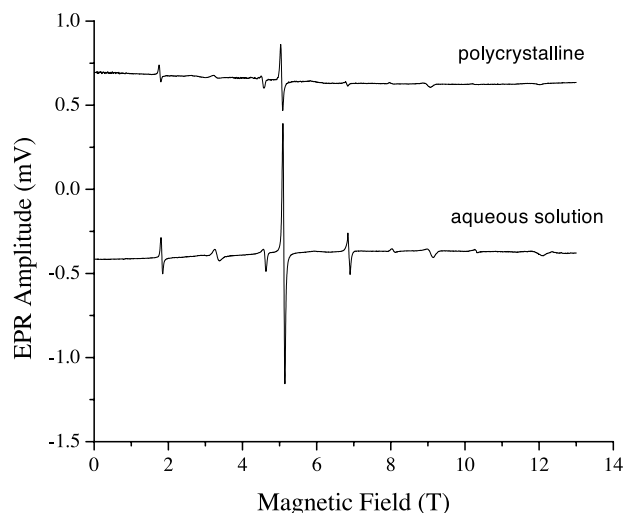


Figure 1. A 191.52 GHz EPR spectrum of a 14.1 mg sample of MnTSP as a polycrystalline solid (top), and in a 55 mM frozen aqueous solution (bottom). $T=20$ K. The old-generation (non-quasi-optical) spectrometer was used.

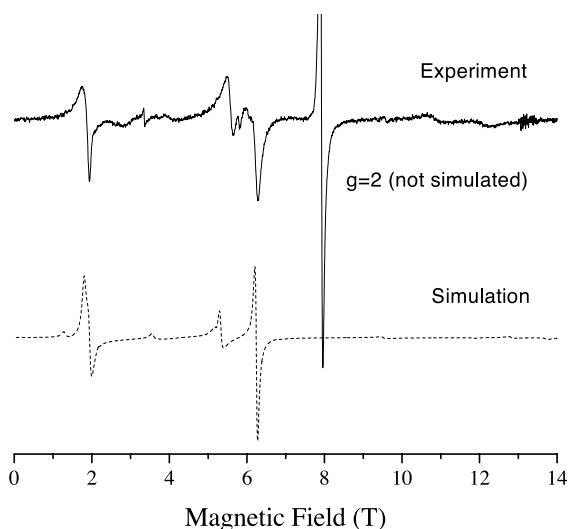


Figure 2. A 220.9 GHz EPR spectrum of a 200 mM $\text{Mn}(\text{acac})_3$ solution in 3:2 CH_2Cl_2 :toluene glass acquired in the quasi-optical spectrometer at $T=20$ K (top), and its simulation (bottom). The spin Hamiltonian parameters used in the latter required significant zero-field splitting rhombicity and were: $D=+3.8$, $|E|=0.4 \text{ cm}^{-1}$, $g=2.00$ (isotropic).

a comparison of the same amount of polycrystalline MnTSP, and its 55 mM water solution. It turns out that performing the experiment in an aqueous glass not only offers a better spectral shape, but also a gain in absolute sensitivity. As for concentration sensitivity, the limit for $S/N=1$ ratio and the strongest spectral feature is about $100 \mu\text{M}$ for the old-generation, direct transmission spectrometer, and about 30 to $50 \mu\text{M}$ for the new quasi-optical setup without optimization

of the non-resonant sample holder. A similar study for non-aqueous solutions of $\text{Mn}(\text{acac})_3$ (Fig. 2), and Jacobsen's catalyst yielded the corresponding values of 1 mM in the old-generation spectrometer, and 300 to $500 \mu\text{M}$ in the new quasi-optical arrangement. We have, therefore, proved it possible to perform HF-EPR experiments on sub-millimolar aqueous and non-aqueous solutions of Mn(III) that are to be expected in biologically-relevant samples.

¹ Telser, J., *et al.*, *Inorg. Chem.*, **37**, 5769 (1998).

² Hagen, W.R., *Coord. Chem. Rev.*, **190-192**, 209 (1999).

³¹P NMR Study of Phase Transitions in KTiOPO_4

Lee, C.E., Korea Univ., Physics

Dalal, N.S., NHMFL

Fu, R., NHMFL

KTiOPO_4 (KTP) is an important electro-optical material with a rare combination of pyroelectricity and superionic conductivity. In our previous ³¹P NMR relaxation study, phase transition behaviors around 200 K and 300 K , associated with a superionic transition and the creation of polarons, respectively, were manifest.¹ In order to further elucidate the nature of these phase transitions, high resolution ³¹P NMR measurements of the chemical shifts employing a 600 MHz superconducting magnet at the NHMFL were planned and carried out.

In accordance with the crystallographic structure of KTP, two resonance peaks were obtained in the MAS (magic angle spinning) spectrum. The two chemical shifts were found to have distinct temperature dependences, as shown in Fig. 1. While they showed very similar slopes in the temperature dependence around room temperature where the phase transition associated with the polaron creation was observed, the slopes had reversed relative magnitudes below and above the room temperature region. This indicates that lattice deformation associated with the polaron creation changes the local environments of the two ³¹P sites. This work thus is a nice demonstration that the state-of-the-art facilities at the

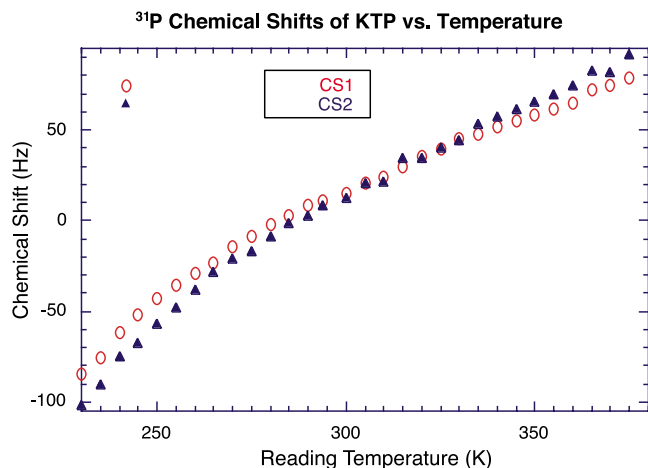


Figure 1. Plot of ^{31}P isotropic chemical shift of KTiOPO_4 (KTP) vs. temperature. The ^{31}P CPMAS measurements were carried out on a Bruker DMX 600 NMR spectrometer and the chemical shift was referenced with respect to $\text{NH}_4\text{H}_2\text{PO}_4$ (ADP). At 305 K, two distinct ^{31}P peaks were observed at 20.6 Hz (CS1) and -258.1 Hz (CS2). In order to compare the temperature dependence of the chemical shifts, the chemical shift of the peak CS2 was shifted by 278.7 Hz at all temperatures. Thus the positions of the CS1 and CS2 in the plot become overlapped at 305 K.

NHMFL can yield previously unavailable information on the microscopic environments in solids.

¹ Lee, C.E., *et al.*, Phys. Rev. B, **55**, 2687 (1997).

Resolution Enhancement in Solution NMR on the Keck Magnet by Intermolecular Zero-Quantum Detection and Matrix Pencil Estimation

Lin, Y.-Y., Princeton Univ., Chemistry
 Warren, W.S., Princeton Univ., Chemistry
 Brey, W., NHMFL
 Murali, N., NHMFL

Strong magnetic fields are desirable in high-resolution NMR to enhance resolution, improve sensitivity, and simplify spectra. Resistive, or hybrid magnets can achieve substantially higher fields than those available in superconducting magnets, but their spatial homogeneity and temporal stability are unacceptable for high-resolution applications. We showed that modern stabilization and shimming

technology produce a sufficiently good field that detection of intermolecular zero-quantum coherences (iZQCs),¹⁻³ using the CPMG-HOMOGENIZED sequence, can remove almost all of the rest of the inhomogeneity, while retaining the information of chemical shift differences and J couplings.⁴ In the 25 T Keck electromagnet (1 kHz/s drift, 3 kHz linewidth over 1 cm^3), preliminary results of iZQC detection of a 1:1 acetone:water solution remove $>99\%$ of the remaining inhomogeneity to achieve a resolution enhancement of ~ 100 , thereby generating the first ever high-resolution, liquid-state NMR spectra acquired at > 1 GHz. Optimization of the pulse sequence and spectrometer promises even higher resolution, until reaching a theoretical boundary of ~ 4 Hz line-width. This motivates, for example, refinement of the flux stabilizer and application of pulse shaping.

iZQC detection is a two-dimensional acquisition scheme, with the high-resolution information encoded in the indirect dimension. The final achievable resolution is restricted by Fourier transforming the heavily truncated signal in the indirect dimension due to limited capacity of cooling water and, therefore, magnet time available for uninterrupted acquisitions. This inherent limitation can be alleviated by invoking high-resolution spectral estimators as alternatives to the Fourier transform. In particular, the method proposed in Ref. 5 is especially promising for estimating and quantifying the iZQC signals. The number of exponential components in the signals is first determined by criteria derived from information theory and the spectral parameters are then estimated by the efficient matrix pencil method. Fig. 1 shows the iZQC spectrum of a 1:1 methyl-ethyl-ketone:water solution processed by the information theory and matrix pencil method. The iZQC spectrum shows the expected peaks at the precise frequency difference with correct phase alternation. More importantly, the J -splitting structures are now resolvable. It may be concluded that the combined detection-estimation scheme provides the possibility of extracting accurate linewidth information in the presence of field instability and inhomogeneity in the Keck magnet.

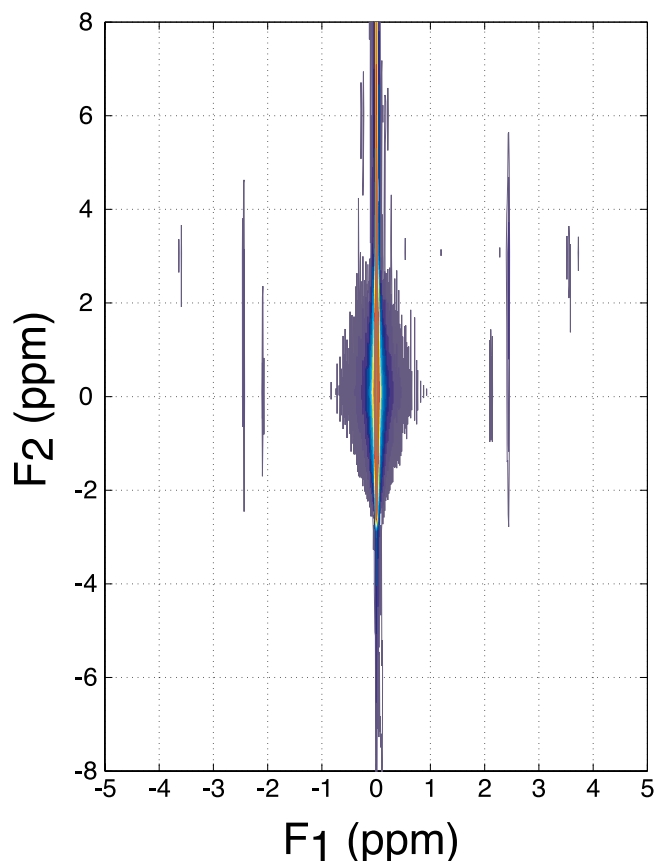


Figure 1. Experimental iZQC spectrum of a 1:1 methyl-ethyl-ketone:water solution detected by CPMG-HOMOGENIZED sequence, and estimated by information theory and matrix pencil method.

Such capability is crucial to our implementation of iZQC variants of the TROSY experiment to verify the theoretical prediction of destructive interference between chemical-shift-anisotropy and dipole-dipole relaxations within ^{15}N - ^1H moieties at very high fields.

Acknowledgements: This work was supported by the NIH under grant GM35253 and the NHMFL.

¹ Warren, W.S., *et al.*, *Science*, **262**, 2005 (1993).

² Lee, S., *et al.*, *J. Chem. Phys.*, **105**, 874 (1996).

³ Vathyam, S., *et al.*, *Science*, **272**, 92 (1996).

⁴ Lin, Y.-Y., *et al.*, *Phys. Rev. Lett.*, **85**, 3732 (2000).

⁵ Lin, Y.-Y., *et al.*, *J. Magn. Reson.*, **128**, 30 (1997).

Toward the NMR Solution Structure of CFBF-SMMHC

Lukasik, S.M., Univ. of Virginia, Chemistry

Bushweller, J.H., Univ. of Virginia, Molecular

Physiology and Biological Physics, and Chemistry

Core Binding Factor (CBF) is a heterodimeric transcription factor which plays a central role in several developmental processes, particularly hematopoiesis. CBF consists of two subunits: CBFA, which binds the asymmetric DNA sequence PyGPyGGT, and CFBF, a non-DNA binding subunit.^{1,2}

Two of the four genes that encode for CBF subunits have been identified as proto-oncogenes commonly altered in human leukemias. Chromosomal translocations involving CBF subunits are associated with 30% of *de novo* acute myeloid leukemias (AML).³ In particular, the pericentric chromosomal inversion [inv(16)(p13;q22)] of the *CBFB* gene produces a chimeric fusion protein which contains the N-terminal 165 amino acid residues of CFBF fused to the coiled-coil tail region of smooth muscle myosin heavy chain (SMMHC).⁴ This protein has been demonstrated to block normal CBF functioning in a transdominant manner.^{4,5}

The goal of this project is to determine the NMR solution structure of a functional portion of the CFBF-SMMHC protein. Our current focus has been on the completion of sequential backbone resonance assignments. Assignments in the SMMHC tail region of the onco-protein have been difficult due to spectral crowding and the repetitive nature in the amino acid sequence. To provide unique starting points, we have utilized ^{15}N specifically labeled samples of valine, leucine, alanine, and phenylalanine. In order to complete the remainder of the assignments, we collected a TROSY based HNCA, and a ^{15}N -edited NOESY spectra on a (^{15}N , ^{13}C , ^2H) labeled CFBF-SMMHC sample at 720 MHz in mid-November 2000. Currently, this data in conjunction with data previously collected at 600 MHz, has allowed for the assignment of approximately 80% of backbone resonances. An example of backbone sequential

High Field ^{27}Al MAS NMR of Zeolite MCM-22

Ma, D., State Key Laboratory of Catalysis, Dalian Institute of Chemical Physics

Fu, R., NHMFL

Han, X., State Key Laboratory of Catalysis, Dalian Institute of Chemical Physics

Bao, X., State Key Laboratory of Catalysis, Dalian Institute of Chemical Physics

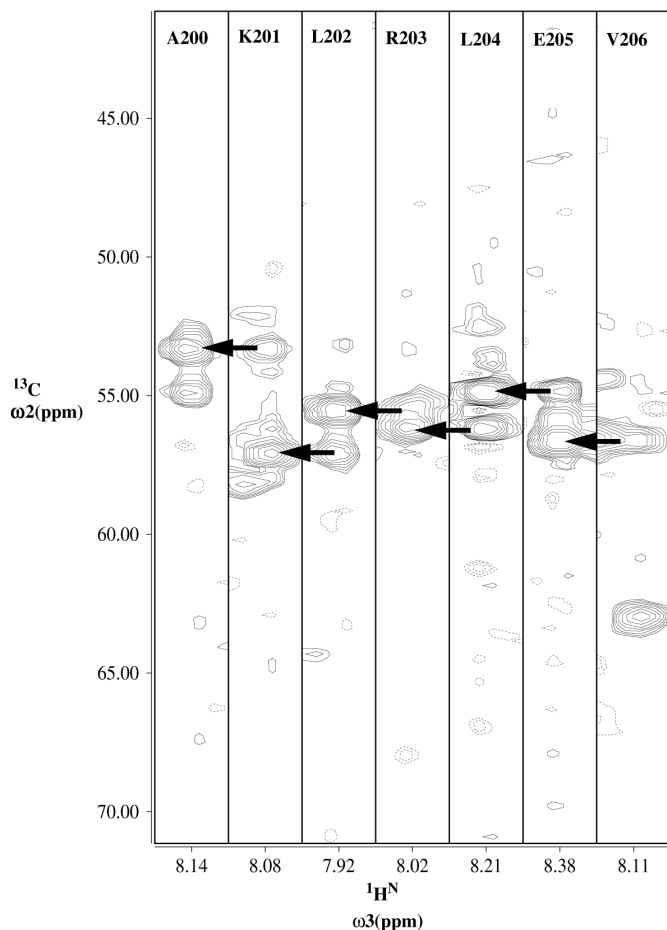


Figure 1. Selected strips from the TROSY-based HNCA spectrum of (^{15}N , ^{13}C , ^2H)-CBFB-SMMHC.

assignments for the HNCA spectrum collected at the NHMFL is demonstrated in Fig. 1.

¹ Melnikova, I., *et al.*, *J. Virol.*, **67**, 2408 (1993).

² Wang, Q., *et al.*, *Cell.*, **87**, 697 (1996).

³ Look, A.T., *Science*, **278**, 1059 (1997).

⁴ Liu, P., *et al.*, *Science*, **261**, 1041 (1993).

⁵ Castilla, L.H., *et al.*, *Cell.*, **87**, 687 (1996).

Zeolite MCM-22,^{1,2} which possesses an unusual crystalline structure—combining the behavior of both the 10 MR and 12 MR systems, has been paid much attention for its prospects in many catalytic reactions. It is well known that the properties and the performance of zeolites usually depend on the state of the aluminum species in the zeolites and, therefore, the investigation of the state of aluminum is significant and interesting. Moreover, MCM-22 is reported to have a special character in its distribution of both Si and Al site.³ Thus, it is valuable to investigate above mentioned issues together with what happened in the dealumination process of MCM-22, and its difference with other zeolites.

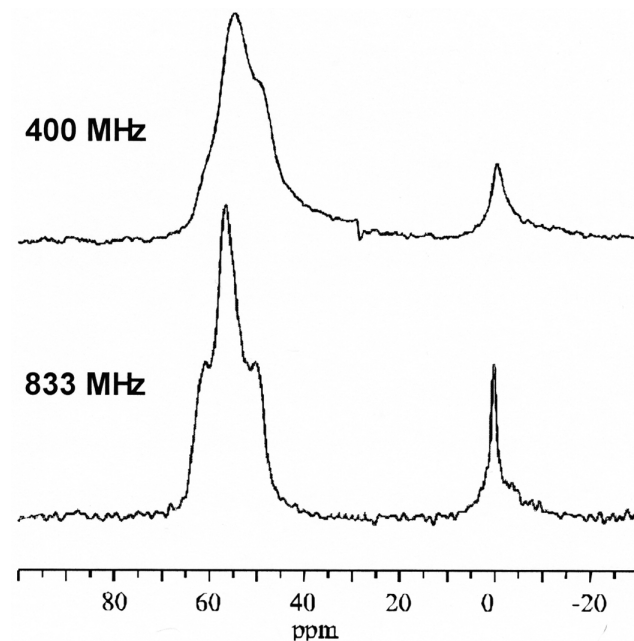


Figure 1. ^{27}Al MAS NMR spectra of MCM-22 at 9.4 T (a) and 19.6 T (b).

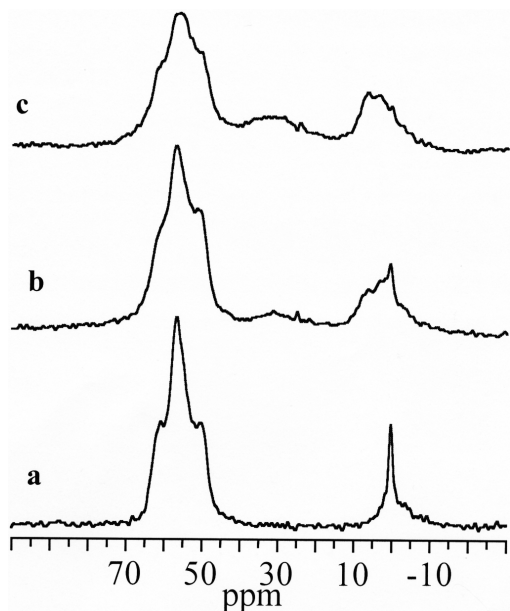


Figure 2. ^{27}Al MAS NMR spectra (19.6 T) of MCM-22 (a) and those dealuminated at 723 K (b) and 823 K (c).

The ^{27}Al MAS NMR spectra (9.4 T) of parent MCM-22 have at least three resonances at 55, 50 and 0 ppm (see Fig. 1). The former two can be ascribed to zeolitic tetrahedral aluminum species, while the latter was octahedral aluminum species. With the field increase to 19.6 T, the lines are narrowed, indicating the removal of the second order quadrupolar effect. At the same time, the shoulder peak at about 60 ppm can be clearly resolved in the 19.6 T spectra. The lines with different chemical shifts can be correlated with different T site in the zeolite.

After dealumination (Fig. 2b and c), the line at 55 ppm, which corresponds to T1, T3, T4, T5 and T8 sites, is preferentially decreased, indicating that the aluminum at those sites is relatively easy to expel from the zeolite lattice. Meanwhile, an additional broad peak appears near 0 ppm, overlapping with the narrow one. The former are proved to be extra framework octahedral aluminum species, whereas, the latter is framework octahedral aluminum species, which can be converted to framework tetrahedral species under specific conditions.

¹ Rubin, M., *et al.*, U.S. Patent 4 954 325 (1990).

² Leonowicz, M.E., *et al.*, *Science*, **264**, 1910 (1994).

³ Kennedy, G.J., *et al.*, *J. Am. Chem. Soc.*, **116**, 11000 (1994).

Single Crystal EPR Studies of the Fe_8 Single Molecule Magnet

Maccagnano, S., Montana State University, Physics
Achey, R., NHMFL

Negusse, E., MSU, Physics

Lussier, A., MSU, Physics

Mola, M., MSU, Physics

Hill, S., MSU, Physics

Dalal, N.S., NHMFL/FSU, Chemistry

Using a high sensitivity cavity perturbation technique,¹ we are able to obtain high field/frequency (up to 9 T/210 GHz) EPR spectra for oriented single crystals of $[\text{Fe}_8\text{O}_2(\text{OH})_{12}(\text{tacn})_6]\text{Br}_8 \cdot 9\text{H}_2\text{O}$ (or Fe_8 for short). Fig. 1 shows representative spectra obtained with the field oriented parallel (a) and perpendicular (b) to the magnetic easy axis. Extrapolating the frequency dependence of transitions to zero-field (for any orientation of the field) allows us to directly, and accurately (to within 0.5%), determine the first five zero-field splittings, which are in reasonable

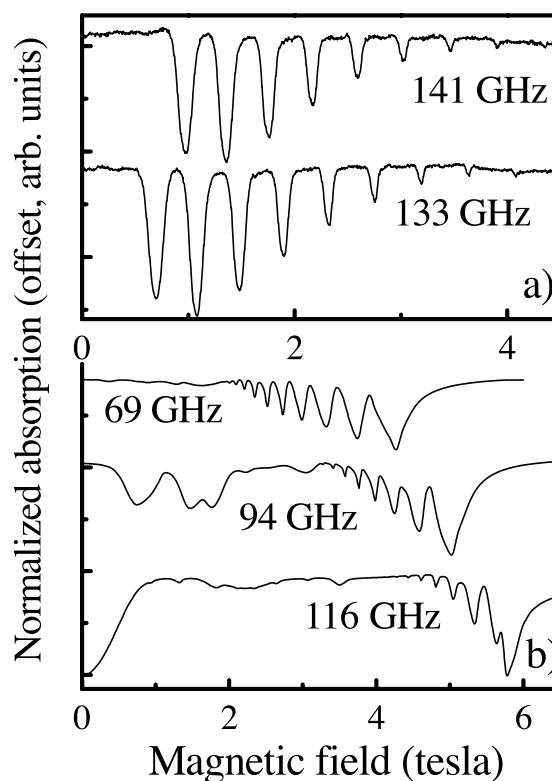


Figure 1. Raw single crystal EPR spectra obtained with the magnetic field applied parallel (a) and perpendicular (b) to the magnetic easy axis.

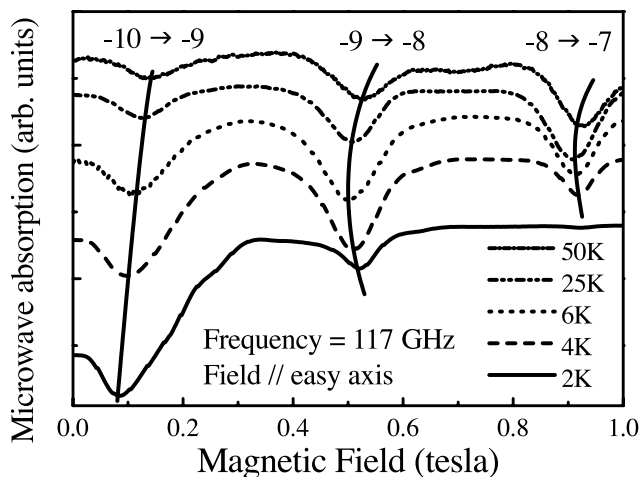


Figure 2. Temperature dependence of data obtained with the field parallel to the easy axis.

agreement with recent inelastic neutron studies.² The dependence of these splittings on the applied field strength, and its orientation with respect to the crystal, enables us to identify (to within 1°) the easy, intermediate, and hard magnetic axes. Subsequent analysis of EPR spectra for field parallel to the easy axis yields a value for g_z that is appreciably different from the value assumed in a recent high field EPR study by Barra *et al.*³ Frequency dependent data obtained for a field applied along the hard and intermediate axes further constrain the g -tensor and spin Hamiltonian parameters up to fourth order.

Analysis of individual resonances, which we can assign to known transitions, reveals a pronounced M_s dependence of the resonance line widths. Furthermore, the line positions exhibit complex (again M_s dependent) temperature dependences (as shown in Fig. 2) that cannot be reconciled with the standard spin Hamiltonian.^{2,3}

Acknowledgements: This work was supported by the Petroleum Research Fund (American Chemical Society).

¹ Mola, M.M., *et al.*, *Rev. Sci. Instrum.*, **71**, 186 (2000).

² Caciuffo, R., *et al.*, *Phys. Rev. Lett.*, **81**, 4744 (1998).

³ Barra, A.L., *et al.*, *cond-mat/0002386* (Feb, 2000).

Perspectives of Solid State NMR for Material Sciences at Very High Magnetic Fields

Massiot, D., CRMHT-CNRS, France

Gan, Z., NHMFL

Quadrupolar nuclei with half-integer spins ($I=n/2$; $n=3,5,\dots$) are of major interest for material sciences. These nuclei are typically light nuclei, both anions and cations, and their solid state NMR spectra are often severely broadened by the second-order quadrupolar effects. The second-order quadrupolar effect is proportional to the inverse of the main magnetic field. Consequently, resolution and sensitivity enhancements are expected to be proportional to the square of magnetic field.¹ We recently demonstrated that at 25 T (~ 1 GHz ^1H frequency), four different sites (Al_{IV} , 2 Al_{V} and Al_{VI}), in the crystalline sample A_9B_2 ($9\text{Al}_2\text{O}_3+2\text{B}_2\text{O}_3$) can be resolved.² Although that kind of resolution can be achieved using more complex two-multidimensional experiments like MQ-MAS³, or the recently described STMAS⁴ techniques, NMR spectra obtained at high field with simple excitation schemes (one pulse and observe) preserve quantitative nature.

The spectra in Fig. 1 show the MAS and static spectra of the disorder-bearing crystalline phase of MgAl_2O_4 and its soft chemistry amorphous precursor. At 25 T, the three types of Al environments (Al_{IV} , Al_{V} , Al_{VI}) present in the amorphous precursor are completely resolved and can be quantified by a simple integration of the ^{27}Al 20 kHz MAS spectrum. At lower magnetic fields, these peaks are overlapped.⁵ It is remarkable that at 25 T magnetic field the static spectra are partially resolved. This example gives a clear illustration of the high spectral resolution offered by high magnetic fields for application of solid state NMR to material sciences.

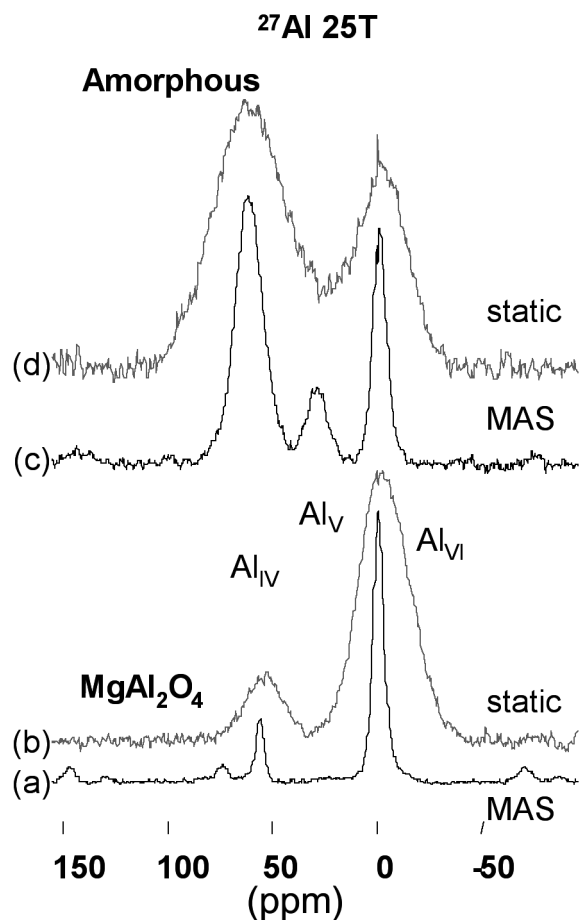


Figure 1. Static and MAS ^{27}Al spectra of crystalline phase MgAl_2O_4 (bottom) and its precursor (top).

- ¹ Massiot, D., *et al.*, C.R. Acad. Science Paris, 157-162 (1998).
- ² Massiot, D., NHMFL Annual Research Review, page 41 (1999).
- ³ Vosegaard, T., *et al.*, Chem. Phys. Lett., **326**, 454 (2000).
- ⁴ Gan, Z., J. Am. Chem. Soc., **122**, 3242 (2000).
- ⁵ Montouillout, V., J. Am. Ceram. Soc. (1999).

The Effect of Radio Frequency Field Inhomogeneity on Heteronuclear Dipolar Recoupling in Solid State NMR; Practical Performance of SFAM and REDOR

Nishimura, K., NHMFL

Fu, R., NHMFL

Cross, T.A., NHMFL/FSU, Chemistry and Institute for Molecular Biophysics

Interatomic distances represent one of the important constraint types for characterizing macromolecular

structure. Thus, it is very important to reveal the reliability and imperfections in methods used to determine the interatomic distances. In the current study, the practical heteronuclear dipolar recoupling performance under magic angle spinning (MAS) conditions for SFAM¹ and REDOR², has been investigated under well-defined rf inhomogeneity environments with a variation of resonance offset for the irradiated nucleus. The heteronuclear dipolar recoupling efficiencies for SFAM and REDOR were quantitatively determined based on the experimentally obtained rf homogeneity.

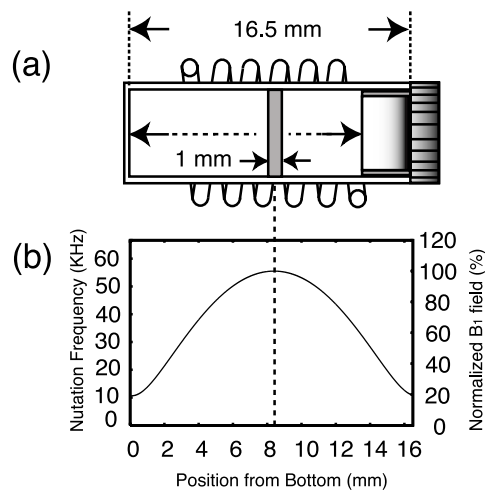


Figure 1. (a) Schematic representation of 1.0 mm thickness rubber disk positioned within the Bruker 7 mm o.d. spinner with a solenoid coil. The solenoid coil length, i.d., and o.d. were 9.3, 7.3, and 8.5 mm, respectively. (b) Position dependent effective rf field variation profile.

The rf inhomogeneity profile for the Bruker 7 mm o.d. triple resonance MAS probe was determined, as shown in Fig. 1, based on the following method. A ^{13}C methyl signal in a rubber disk was observed at 13 positions from the bottom to the top of the spinner. The peak integrals were translated into an rf homogeneity profile based on an equation that described the relationship between the resonance integral and net nutation field.

After the rf inhomogeneity profile was obtained, SFAM¹ and REDOR² experiments were carried out for 3 different sample positions, and 11 different carrier offset frequencies. The experimental heteronuclear dipolar recoupling efficiency with respect to the rf inhomogeneity and rf carrier offset was obtained as contour maps (Fig. 2). Consequently, SFAM retained

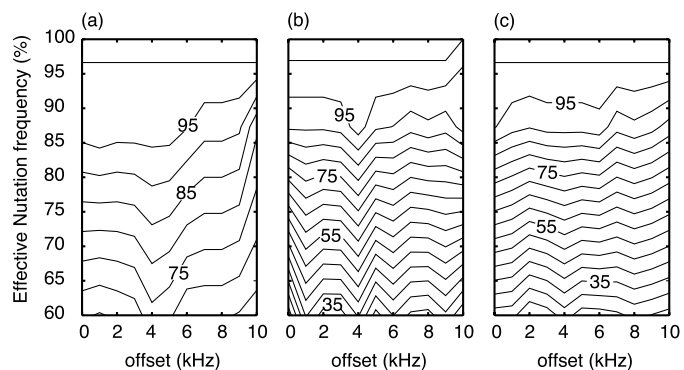


Figure 2. The contour maps for experimental heteronuclear dipolar recoupling efficiencies as a function of rf inhomogeneity and carrier frequency offset for irradiated nucleus for (a) SFAM, (b) REDOR with XY-8, and (c) with XY-16 compensation. The Z axis is dipolar recoupling efficiency (%). Each contour map is drawn based on 33 experimental pairs of carrier frequency offset and sample position values.

a higher recoupling efficiency (>95%) at an effective nutation frequency greater than 85%. The recoupling efficiency is gradually reduced at lower effective nutation frequencies. On the other hand, REDOR with XY-8 compensation pulse sequence, showed an increased sensitivity to nutation frequencies less than 90%. Over all, SFAM had advantages for insensitivity to carrier frequency offset and rf inhomogeneity.

Acknowledgements: The authors thank Dr. William Brey for useful discussion about rf inhomogeneity.

¹ Fu, R., *et al*, Chem. Phys. Lett., **272**, 361-369 (1997).

² Gullion, T., *et. al*, J. Magn. Reson., **81**, 196-200 (1989).

Electrically Detected ENDOR and DNP in a Two-Dimensional Electron System at n=1

Olshanetsky, E., UF, Chemistry
 Bowers, C.R., UF, Chemistry
 Simmons, J.A., Sandia National Laboratories
 Reno, J.L., Sandia National Laboratories

The Overhauser effect, first observed and explained in metals, is the enhancement of the nuclear spin magnetization due to saturation of the electron spin polarization by a resonant microwave field.

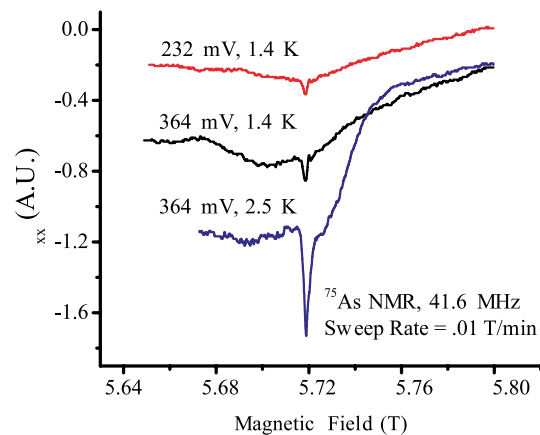


Figure 1. Electrically detected ENDOR detection of arsenic-75 NMR in GaAs/AlGaAs multiple quantum wells at unit filling factor for two different microwave powers (proportional to the indicated detector voltage) and at two temperatures.

Relaxation of the electron spins is assisted by angular momentum transfer to the nuclei. These phenomena have been reported in alkali metal atom vapors and in 2D electron gases (2DEG's), such as in doped GaAs quantum wells.¹

In GaAs quantum wells, the Overhauser enhancement of the nuclear spin polarization can in turn produce an observable Overhauser shift of the ESR via the hyperfine field. Overhauser shift detection of NMR in doped GaAs quantum wells is a double resonance phenomenon involving the interruption of the Overhauser effect when nuclei in the vicinity of the 2D electron gas come into resonance with the applied radio frequency field. Here, we report that the destruction of nuclear polarization by NMR can be detected as a change in magnetoresistance in such a way that the electron spin resonance condition is not lost, and moreover, the NMR response is acquired with high resolution. We have characterized this NMR response under varying conditions of temperature and microwave power, as shown in the figure, with the purpose of understanding the detection mechanism and to determine its relationship to the actual NMR absorption.

In the magnetoresistance detection mode, the ESR signal manifests itself as a sharp resonance feature. Our results demonstrate that, for sufficiently slow

field sweeps, the spin resonance feature is sharp and narrow for magnetic field up-sweeps, but smeared out and deepened for down-sweeps. The variations in EDESR line shape results from the interplay between DNP and the Overhauser shift. The cross-relaxation rate seems to be very sensitive to temperature in the 0.5 to 2 K range. The cross-relaxation rate is directly related to the speed at which the excess energy deposited by the microwave field can be absorbed by the electron system. The temperature dependence of the spectral density of the fluctuations in the hyperfine interaction provides a previously uninvestigated window on the electron spin dynamics and electron-nuclear interactions in a 2DEG.

¹ Berg, A., *et al.*, Phys. Rev. Lett., **64**, 2563 (1990).

Rapid Analysis of Non-Uniformly Sampled Pulsed Field Gradient MRI Data for Velocimetry ▽IHRP▲

Raghavan, K., FAMU-FSU College of Engineering and NHMFL
Park, J.C., FAMU-FSU COE and NHMFL
Gibbs, S.J., FAMU-FSU COE and NHMFL

We have implemented Bretthorst's recent¹ generalization of the Lomb-Scargle periodogram for frequency estimation for non-uniformly sampled, complex data with an arbitrary decay for the problem of velocity estimation from non-uniformly sampled pulsed field gradient MRI data. The method involves recursive windowing of the raw data and calculation of the peak velocity (frequency) in the generalized Lomb-Scargle periodogram to arbitrary precision. The method is an improvement over our previous work^{2,3} in speed and ability to deal with arbitrary decays (for example non-Gaussian spectra of velocities for an individual pixel). Computation times for a 128x128 image with on the order of ten q (motion encoding wave vector) samples are on the order of 10 seconds for velocity precision of better than 0.1% using a 500 MHz Pentium computer. The algorithm is currently

being used for our velocity measurements, and a manuscript is in preparation for publication.

Acknowledgements: This work was supported in part by the NHMFL In-House Research Program and the FAMU-FSU College of Engineering.

-
- ¹ Bretthorst, G.L., to appear in Maximum Entropy and Bayesian Methods, Ali-Mohammad-Djafari (ed), Kluwer (2000).
² Xing, D. *et al.*, Journal of Magnetic Resonance, **106**, 1-9 (1995).
³ Raghavan, K., MS thesis, FSU (2000).

Inductive Shield Magnetic Field Stabilization for NMR in Bitter Magnets

Sigmund, E.E., Northwestern Univ., Physics and Astronomy
Mitrovic, V.F., Northwestern Univ., Physics and Astronomy
Calder, E.S., Northwestern Univ., Physics and Astronomy
Thomas, G.W., Northwestern Univ., Physics and Astronomy
Halperin, W.P., Northwestern Univ., Physics and Astronomy
Reyes, A.P., NHMFL
Kuhns, P.L., NHMFL
Moulton, W.G., NHMFL

In previous NMR measurements,¹ we have demonstrated the apparent decoherence in a signal-averaged NMR experiment due to the magnetic field instability² of a Bitter magnet. In this report, we describe progress in the suppression of this phase noise by inductive shielding of the AC components of the applied magnetic field using a highly conducting aluminum tube. We performed ¹³C NMR on a fully (99%) ¹³C-substituted glycerol sample (glycerol-¹³C₃), in an applied field of 16.4 T.

We fabricated a high-quality, high-conductivity, cylindrical aluminum shield in which we placed our sample and NMR coil. Since the conductivity of the shield improves at lower temperatures, we decreased the shield temperature to demonstrate improved shielding while holding the sample at 295 K.

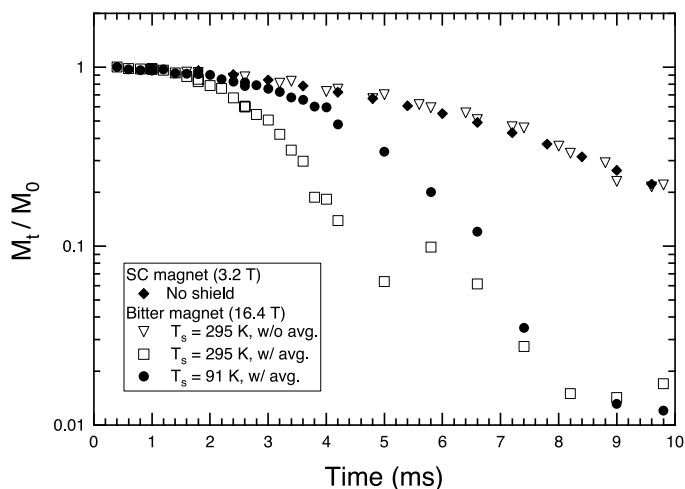


Figure 1. ^{13}C NMR Hahn echo decays in glycerol- $^{13}\text{C}_3$ for two magnet types, different shield temperatures, with and without signal averaging.

Fig. 1 shows transverse decays in a Hahn echo experiment comparing a stable superconducting magnet and the resistive Bitter magnet. Phase decoherence due to the Bitter magnet instability is evident through degradation of the signal with signal averaging. The comparison of the data sets for shield temperatures of 295 K and 91 K shows, unambiguously, a reduction of the phase error with the signal amplitude approaching the intrinsic behavior mapped out in the low field stable superconducting magnet. In Fig. 2, we show “residual” decays of the shielded profiles obtained by dividing out the intrinsic decay. We find the leading order behavior of these decays to be quartic, in agreement with our analysis of earlier experiment and theory of the phase noise from a harmonic field instability.¹ The fit results to this form indicate a shielding factor of $S=0.42\pm 0.05$ at a shield temperature of 91 K. This result is quantitatively consistent with NMR measurements that we have made with the same shield, but with externally applied field fluctuations at 60 Hz. Based on this prior experience at different shield temperatures, we can extrapolate to 4 K to expect a shielding factor of more than two orders of magnitude if the shield can be maintained at 4 K in the Bitter magnet.

Acknowledgements: This work was supported by NSF-MRSEC through the Materials Research Center at Northwestern University, grant DMR-0076097.

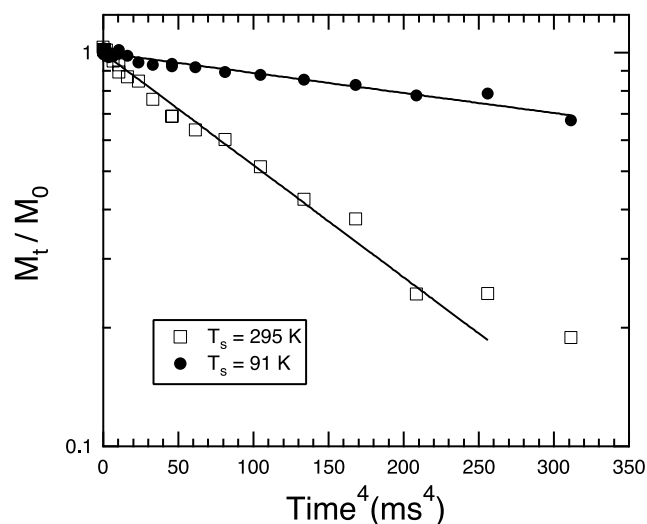


Figure 2. Residual ^{13}C NMR Hahn echo decays in glycerol- $^{13}\text{C}_3$ (intrinsic decay removed) for two shield temperatures.

- ¹ Sigmund, E.E., *et al.*, Journal of Magnetic Resonance, in press.
- ² Soghomonian, V., *et al.*, Review of Scientific Instruments, **71**, 2882-2889 (2000).

The Stochastic Liouville Equation in Magnetic Resonance: An Object Oriented Implementation

Smith, S.A., NHMFL
 Khairy, K., NHMFL/Northeastern Univ.,
 Chemistry
 Fajer, P., NHMFL/FSU, Biological Sciences
 Budil, D., Northeastern Univ., Chemistry

Magnetic resonance (MR) is arguably the best method for investigating molecular dynamics. In all but the simplest of cases, such explorations are inevitably achieved through an iterative fit of simulated spectra to acquired data. Considering the multitude of experimental difficulties, the increasingly complex systems under study, and the formidable theory required to describe spin dynamics, it is not surprising that such studies are, in general, quite difficult to accomplish. This report describes work that should greatly simplify this process on the computational end *via* the implementation of appropriate theory into a flexible computational environment using modern object oriented programming (OOP) techniques.

In order to facilitate dynamics studies, we have begun including solutions of the stochastic Liouville equation (SLE) into the premier MR simulation platform,¹ GAMMA. Our aim is to provide users with a flexible and expandable framework upon which one may construct MR simulation programs that include relaxation and exchange effects as described by the SLE. The SLE allows for investigations using a wide variety of dynamical pictures, spanning fast through slow motional regimes. The object-oriented approach being taken is not limited to any number of spins nor their spin types and hence can readily handle both NMR and EPR computations. Provisions are being made which allow for internal system flexibility and spin interaction definitions in any number of coordinate frames. This added SLE capability will work seamlessly with the wide arsenal of tools already supplied in the GAMMA platform. Consequently, we will be able to provide an array of software tools that can rigorously treat dynamics problems and, in addition, extend existing treatments so as to handle newly proposed motional models and larger spin systems that have thus far been virtually inaccessible.

The first challenge in treating the SLE is computational size. The stochastic Liouvillian itself is a superoperator (matrix) of very large dimension. Its size grows rapidly with the number of spins being treated, their spin quantum numbers, and the allowed flexibility in the system. Were it not for the fact the superoperator is sparse, most SLE problems would be inherently unapproachable even with modern computer capabilities. Thus, use of sparse matrices is mandatory for dealing with such problems. For the GAMMA OOP platform, this translates into providing: (1) a sparse matrix class that can handle large arrays, (2)² Lanczos diagonalization routines in order to obtain eigensystems of such arrays, and (3) continued fractions algorithms for rapid eigensystem regeneration during field swept (CW ESR/NMR) simulations. In true object-oriented fashion, the typical GAMMA programmer need have no knowledge of such intricacies and may freely use such arrays in combination with any other specialized GAMMA matrix types, independent of the SLE.

With the above difficulty nearly overcome, we will next deal with: (1) producing a module that will iteratively fit experimental data, (2) incorporation of a dynamics interface within a spin system so that internal motions can be easily accommodated, and (3) construction of programs to satisfy our current scientific needs, ultimately making these available to the public.

¹ Smith, S.A., *et al.*, *J. Magn. Reson.*, **106a**, 75-105 (1994).

² Lanczos, C., *J. Res. Nat. Bur. Stand.*, **45**, 255-82 (1950).

Monitoring Formation of the Type II Mixed Hydrate Clathrate by Spin-Exchange Optical Pumping Enhancement of Xenon-129 NMR ▽IHRP▲

Storhaug, V., UF, Chemistry

Bowers, C.R., UF, Chemistry

Spin exchange optical pumping enhancement of xenon-129 NMR is an ideal method for the study of Xe hydrate clathrates over a wide range of reaction conditions. As a consequence of the >1000 fold sensitivity enhancement afforded by this method, the kinetics and mechanism of formation, cavity occupation ratios, geometrical distortions and cavity dynamics can all be studied.

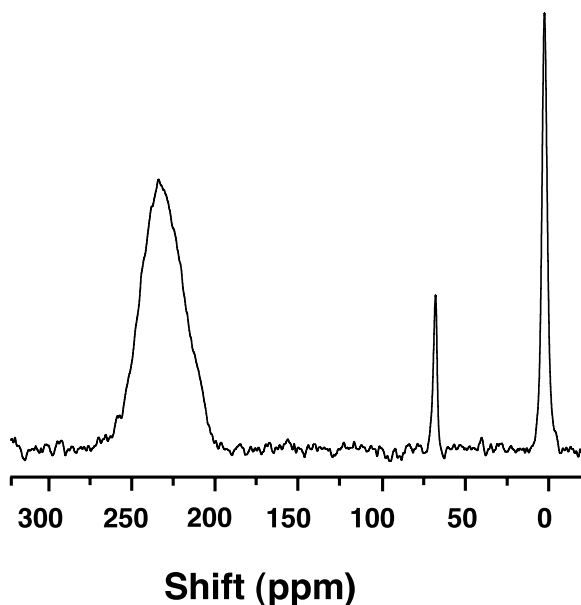


Figure 1. Spin exchange enhanced ¹²⁹Xe NMR spectra (single scan) of the type II SF₆/Xe hydrate clathrate formed at 223 K with SF₆ at 3800 Torr.

We have used spin exchange optical pumping enhancement of xenon-129 NMR to characterize the formation of SF₆/Xe (see Fig. 1) and acetone/Xe mixed type II hydrate clathrates at the comparatively high temperature of 223 K, where it was observed that the enclathration of Xe into a type-II structure occurs on the time scale of several minutes. The spectra show that Xe is excluded from the larger hexakaidecahedral cavities, although the degree of exclusion of Xe from the larger cavities appears

to be more complete in the case of acetone-*d*₆. A comparison of the line shapes associated with the dodecahedral cavities in the acetone-*d*₆ and SF₆ reveals subtle differences in the symmetry of these structures due to differences in shape of these hydrate formers. A difference in the xenon-129 spin lattice relaxation time in the dodecahedral cavities is interpreted in terms of differences in guest-guest intermolecular dipolar interactions.

